JOURNAL OF GEOPHYSICAL RESEARCH, VOL. 106, NO. B6, PAGES 11,115–11,125, JUNE 10, 2001

Statistical analysis of synthetic earthquake catalogs generated by models with various levels of fault zone disorder

Chunsheng Lu [1] and David Vere-Jones

School of Mathematical and Computing Sciences, Victoria University of Wellington
Wellington, New Zealand

Abstract. The stress release model, a stochastic version of the elastic rebound theory, is applied to the large events from four synthetic earthquake catalogs generated by models with various levels of disorder in distribution of fault zone strength (*Ben-Zion*, 1996) They include models with uniform properties (U), a Parkfield-type asperity (A), fractal brittle properties (F), and multi-size-scale heterogeneities (M). The results show that the degree of regularity or predictability in the assumed fault properties, based on both the Akaike information criterion and simulations, follows the order U, F, A, and M, which is in good agreement with that obtained by pattern recognition techniques applied to the full set of synthetic data. Data simulated from the best fitting stress release models reproduce, both visually and in distributional terms, the main features of the original catalogs. The differences in character and the quality of prediction between the four cases are shown to be dependent on two main aspects: the parameter controlling the sensitivity to departures from the mean stress level and the frequency-magnitude distribution, which differs substantially between the four cases. In particular, it is shown that the predictability of the data is strongly affected by the form of frequency-magnitude distribution, being greatly reduced if a pure Gutenburg-Richter form is assumed to hold out to high magnitudes.

1. Introduction

Just as the satellite cloud atlas is important in weather forecasting, the tectonic stress field in the Earth's crust is very important in earthquake prediction. Although we cannot directly get such a map by using present techniques, the tectonic stress pattern within a seismic region can be indirectly inferred from different kinds of information. Among them, historical earthquake catalogs may most directly reflect the nature of earthquake-generating stress. Unfortunately, the usable part of historical data is extremely short, and considerable caution should be taken to assess the completeness of all data sets used. However, using a geophysical model, we can easily produce the so-called synthetic earthquake catalogs, which have some obvious advantages over real earthquake data. They are free of observational errors and can be made as long as needed to obtain good statistical samples. In addition, the underlying models are completely known and controlled [e.g., *Ben-Zion and Rice*, 1993, 1995; *Ben-Zion*, 1996; *Bebbington*, 1997; *Shi et al.*, 1998; *Lu et al.*, 1999b, 1999c]. They provide, therefore, an excellent testing ground for different kinds of statistical modeling and analysis procedures, and for better understanding of the relations between observed patterns of activity and the results of statistical analyses.

The spatio-temporal seismicity patterns in a given region are closely related to both tectonic regime and fault structures. Although such relations may be visually evident in the sequences of both real and synthetic earthquake catalogs, an important problem remains of quantifying the relations in a way which allows large events in the seismic region to be predicted, at least in probabilistic terms. One question we examine here is whether there is a relationship between the degree of predictability and the assumed fault properties. The synthetic catalogs generated by *Ben-Zion* [1996] provide a convenient platform for examining this question. The catalogs show quite different patterns as the fault properties, specifically the character of the heterogeneities in the fault strength, are varied. In this paper, a simple statistical model is fitted to the synthetic catalog data, and the variations in its parameters from case to case are interpreted in terms of the fault properties and visual characteristics of the catalogs. The exercise is

[1] Also at Laboratory of Non-linear Mechanics, Institute of Mechanics, Academia Sinica, Beijing, China.

Paper number 2000JB900452
0148-0227/01/2000JB900452$09.00.

important both in determining the extent to which a simple statistical model can discriminate between the catalogs and in calibrating the model itself. In addition, the degree of predictability of the seismicity in the four different classes of faults is investigated by using simulation techniques based on the fitted statistical models. The results obtained follow the same qualitative sequence as those obtained by *Eneva and Ben-Zion* [1997a, 1997b] using (nonparametric) pattern recognition techniques. One advantage of the present approach is that it also allows the assessment of prediction errors, as, for example, in using simulations to forecast the probability distribution of the time to the next event above a given threshold.

A particular feature of the analysis is that the model was fitted only to the larger events in the different catalogs. Nevertheless, the model fits the data well, suggesting that the smaller events play a relatively minor role in determining the large-scale behavior of the system. The effect of varying the lower stress (magnitude) threshold is examined and provides further insight into the relative roles of smaller and larger events.

2. Stress Release Model

In terms of the elastic rebound theory proposed by *Reid* [1911], stress in a seismically active region accumulates slowly owing to the relative movement across faults. When the stress exceeds a certain threshold, for example, the strength of rock media, an earthquake occurs and the accumulated strain energy is released rapidly generating seismic waves. Although the elastic rebound model and its modifications have been widely used in time-dependent hazard prediction, real sequences of large earthquakes are fundamentally more complicated. Many features of the seismic process are not fully captured in the basic elastic rebound model with a small number of degrees of freedom, producing an apparent randomness which has to be taken into account if the model is to be used for predictive purposes.

Through a development of the Markov model suggested by *Knopoff* [1971], the stress release model, a stochastic version of the elastic rebound theory, was proposed by *Vere-Jones* [1978] and subsequently applied to the statistical analysis of historical earthquake data from China, Japan, and Iran [e.g., *Vere-Jones and Deng*, 1988; *Zheng and Vere-Jones*, 1991, 1994; *Lu et al.*, 1999a]. In this model, a scalar regional stress level $X(t)$ is assumed to increase deterministically between two earthquakes and to be released stochastically as a one-dimensional Markov process. The evolution of stress versus time is assumed to follow the equation

$$X(t) = X(0) + \rho t - S(t), \tag{1}$$

where $X(0)$ is the initial stress level, ρ is the loading rate from external tectonic force, and $S(t)$ is the accumulated stress release from events within the region over the time period $(0, t)$: $S(t) = \sum_{t_i<t} S_i$, where $\{t_i, S_i\}$ are the origin time and stress release associated with the ith earthquake [*Zheng and Vere-Jones*, 1991, 1994].

Kanamori and Anderson [1975] indicated that the magnitude m is proportional to the logarithm of the seismic energy release E during an earthquake, i.e., $m = \frac{2}{3}\log_{10} E + \text{const}$. For simplicity, the stress drop is supposed to be proportional to the Benioff strain release and hence to the square root of the energy release. Thus it is assumed that the stress release S_i during an earthquake with magnitude m_i, relative to a reference event with magnitude m_0, can be calculated by the formula

$$S_i = 10^{0.75(m_i - m_0)}. \tag{2}$$

In the subsequent analysis, $m_0 = 5.0$ is used, both for the reference magnitude and for the lower-threshold magnitude in the catalogs; the substance of the results is not sensitive to the choice of m_0. We refer to *Ben-Zion* [1996] for details on how an equivalent magnitude is ascribed to events from the simulation.

The stochastic behavior of the model is controlled by two factors: a risk function $\Psi(X)$ governing the probability of an event occurring for a given level of stress and the distribution of stress releases $f(m|X)$. In this paper, we choose for $\Psi(X)$ the exponential function $\Psi(X) = \exp(\mu + \nu X)$, where μ and ν represent a background constant and the sensitivity to risk, respectively, and X is given by (1). The choice of the exponential function may be regarded as a compromise between two extreme cases: the time predictable process (corresponding approximately to a 0–1 risk function) and the pure random (Poisson) process. The soft boundary may be regarded as a surrogate for the unknown fluctuations in fault properties in space, and possibly in time, which occur both in real contexts and in the present synthetic catalog models. It is further assumed that the probability distribution of earthquake sizes $f(m|X)$ is independent of the stress level ($f(m|X) = f(m)$) and, as a default, governed by the standard Gutenberg-Richter (GR) law. The adequacy of this last assumption will be examined further in the discussion of the results.

With these simplifying assumptions, the model can be treated as a marked point process with conditional intensity function (instantaneous rate for events with magnitude m, conditioned on the past) of the general form

$$\begin{aligned} \lambda(t, m) &= \Psi[X(t)] f[m|X(t)] \\ &= \exp\{\alpha + \nu[\rho t - S(t)]\} f(m), \end{aligned} \tag{3}$$

where $\alpha = \mu + \nu X(0)$. The interpretation of the parameters α, ν, and ρ will be discussed later. Their estimates can be found by numerically maximizing the log likelihood

$$\log L = \left[\sum_{j=1}^{N} \log \lambda(t_j) - \int_{T_1}^{T_2} \lambda(t)dt\right] + \sum_{1}^{N} \log f(m), \tag{4}$$

where N is the number of events observed in the interval (T_1, T_2) [*Harte*, 1998] and $\lambda(t) = \Psi(X(t))$. In our case, since the risk term $\Psi(X(t))$ and the magnitude term $f(m)$ have no parameters in common, the parts of the likelihood involving $\lambda(t)$ and $f(m)$ can be optimized separately.

The likelihood approach can be extended to making comparisons between models by using the Akaike information criterion (AIC), which is defined as

$$\mathrm{AIC} = -2\log\hat{L} + 2k, \tag{5}$$

where $\log\hat{L}$ is the maximum log likelihood for a given model and k is the number of parameters in the model [*Akaike*, 1977]. This represents a rough way of compensating for additional parameters and is a useful heuristic measure of the relative effectiveness of different models [e.g., *Zheng and Vere-Jones*, 1991, 1994; *Main et al.*, 1999]. For example, in comparing the stress release model with three parameters against the Poisson model with only one ($\nu = \rho = 0$ in (3)), the more complex model must demonstrate a significantly better fit to justify the additional parameters. In typical cases, model differences which would be significant at around the 5% confidence level correspond to difference in AIC values of around $1.5 \sim 2$. The best model is that for which AIC as defined in (5) has the smallest value.

3. Synthetic Catalogs

The catalogs we use in this paper were generated by *Ben-Zion* [1996] based on earlier models of *Ben-Zion and Rice* [1993, 1995]. Their models simulate seismicity along a fault segment 70 km long and 17.5 km deep. The fault is divided into square cells with dimension of 550 m. The boundary conditions and model parameters are compatible with observations along the central San Andreas fault. The slip history in each model realization is calculated for 150 years. In the model of *Ben-Zion* [1996], each fault position can sustain both creep and brittle failures. All model realizations are characterized by the same creep properties chosen to produce realistic stress envelope with depth, but their brittle properties vary to simulate the following four cases. These are a uniform background distribution with small uncorrelated random fluctuations (model U); a case with a Parkfield-type asperity of size 25 km × 5 km (model A); a fractal (power law) distribution of brittle properties with fractal dimension 2.3, mean value 0.5, and standard deviation 0.2 (model F); and a distribution with multi-size-scale heterogeneities (model M). The assumed distributions represent two idealized situations: a strongly disordered state representing immature fault zones and extended spatial domains and a relatively regular state representing mature highly slipped faults [see *Ben-Zion*, 1996]. The models produce several types of output, one of which is synthetic earthquake catalogs that are used here. In each case, the stress release is mainly due to large- and medium-magnitude earthquakes. For the present analysis, the synthetic catalogs were first restricted to events with a magnitude threshold $m \geq 5.0$. A second analysis was then carried out with the threshold dropped to $m \geq 4.5$. Even in the latter case the number of events used represents only a small proportion (about 1%) of the events in the original catalog. To avoid problems with transient effects at the beginning of the simulation, data fitting was carried out on the last 100 "years" of the catalog history (years 200–300 in the following figures).

4. Results and Discussion

Two kinds of basic statistical models, the Poisson model and the stress release model, were applied to the analysis of the synthetic catalogs mentioned above. These two models represent two contrasting cases: the pure random process and a simplified (one-dimensional stress) pseudo-periodic process. We shall examine the results of fitting these models under three headings: general features and model sequencing, comparison and interpretation of parameter values, and predictability.

Table 1. AIC Values Calculated by Using the Stress Release Model (AIC_s) to the Synthetic Catalogs Generated by Models with Various Levels of Fault Zone Disorder[a]

Model	m_{th}	N	AIC_s	AIC_p	ΔAIC	$\Delta\mathrm{AIC}/N$
U	5.0	30	77.22	134.24	-57.02	-1.90
	4.5	211	61.95	108.90	-46.95	-0.22
F	5.0	28	97.07	129.28	-32.21	-1.15
	4.5	268	-114.02	9.60	-123.62	-0.46
A	5.0	51	142.82	172.68	-29.86	-0.59
	4.5	263	-11.51	19.37	-30.88	-0.12
M	5.0	67	163.14	189.66	-26.52	-0.40
	4.5	358	-222.61	-195.16	-27.45	-0.08

[a]U, uniform properties; F, fractal brittle Properties; A, Parkfield-type asperity; and M, multi-size-scale heterogeneities; m_{th} is the threshold magnitude, AIC_p represents the AIC value calculated by the Poisson model, $\Delta\mathrm{AIC} = \mathrm{AIC}_s - \mathrm{AIC}_p$, and N is the number of events

4.1. General Features and Model Sequencing

As was discussed above, the relative effectiveness of different models in fitting the data can be determined by the difference of AIC values, for example, $\Delta\text{AIC} = \text{AIC}_s - \text{AIC}_p$, where AIC_s and AIC_p are the AIC values calculated for the stress release model and the Poisson model, respectively. These values are shown for the four models in Table 1. The first of each pair of rows refers to the analysis with magnitude threshold $m \geq 5$ and the second refers to the analysis with $m \geq 4.5$. Note that this table refers only to the first term of the log-likelihood in (4), namely, that relating to the time sequence of the points, the magnitude assumptions being the same for both models.

In all cases, the stress release model fits the data better than the Poisson model, and in all cases the differences are substantial. If we use the Poisson model as a reference, the values of ΔAIC in the four cases with $m \geq 5$ follow the order U, F, A, and M. However, such a direct comparison might be misleading, as the different catalogs yield different numbers of events. In order to allow for this effect, we use the indicator $\Delta\text{AIC}/N$ as a measure of the improvement in performance which is approximately independent of sample size [e.g., *Kagan and Knopoff*, 1977; *Di Luccio et al.*, 1997]. The larger the negative value of the ratio, the better the seismicity pattern is fitted by the alternative model (i.e., the stress release model) relative to the Poisson model. Thus the values of $\Delta\text{AIC}/N$ give an indication of the degree of periodicity of each catalog, at least in the sense of degree of departure from the Poisson model. They also provide a measure of the increase in predictability for each model over the base level provided by the Poisson model (for the detailed discussion, see *Vere-Jones* [1998]).

For the larger events set ($m \geq 5$), the order in which $|\Delta\text{AIC}/N|$ decreases clearly follows the sequence U, F, A, and M, which is consistent with the sequence obtained by *Eneva and Ben-Zion* [1997a, 1997b] using pattern-recognition techniques. Indeed, the sequence is obvious from a visual comparison of the fitted intensity functions for the four different cases, as is shown in Figure 1. Catalog U is closest to periodic; the others show increasing levels of randomness. It is equally obvious

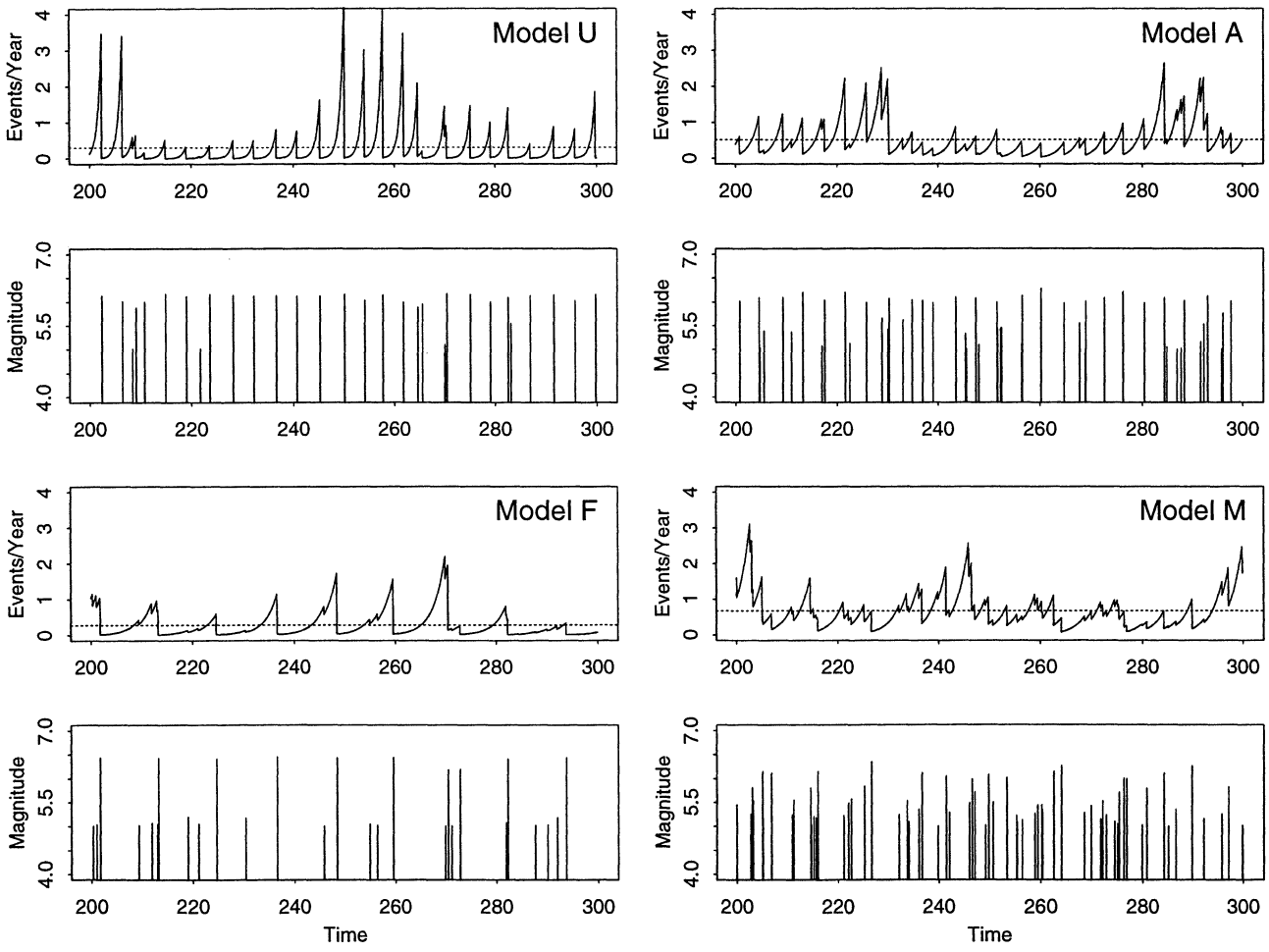

Figure 1. risk function (events/year) versus time (year) for the data with threshold $m \geq 5$ calculated by the stress release model (solid line) and the Poisson model (dotted line). For comparison, the earthquake catalog in each case is also plotted.

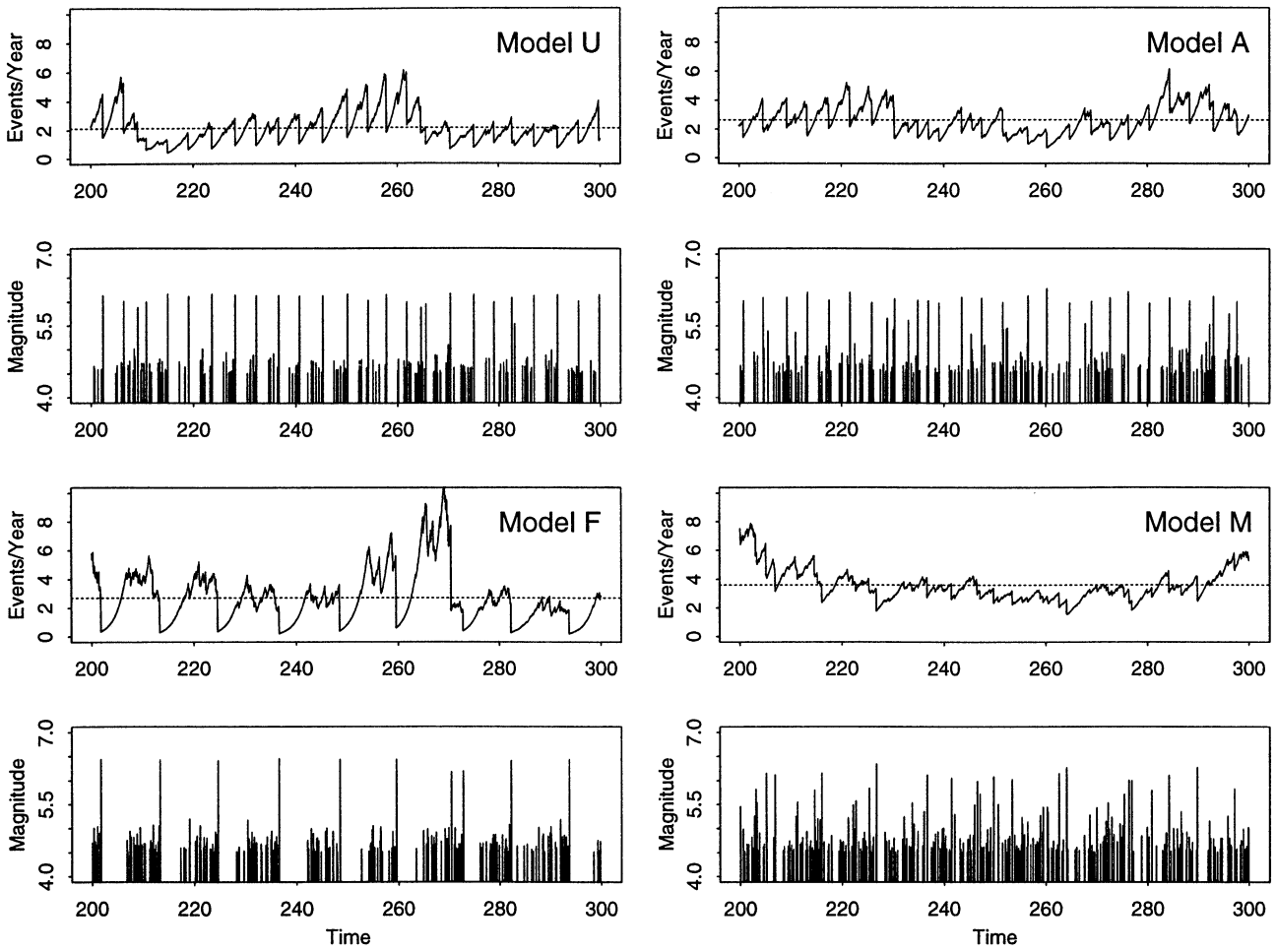

Figure 2. risk function (events/year) versus time (year) for the data with threshold $m \geq 4.5$ calculated by the stress release model (solid line) and the Poisson model (dotted line). For comparison, the earthquake catalog in each case is also plotted.

that the values of $|\Delta\text{AIC}/N|$ are systematically lower for the data with the lower threshold. The implication is that the model is relatively less effective in describing the behavior of the smaller events, which appear to be more randomly located along the time axis. The most interesting case is model F, which shows the biggest decrease in $|\Delta\text{AIC}/N|$ of the four models. Examination of the four plots (Figure 2) shows that there is indeed a striking feature here, namely, the clear gaps after all except the last two large events. Such gaps will be far better fitted by the stress release model than by the Poisson model and will no doubt account for the greater improvement indicated by the value of $|\Delta\text{AIC}/N|$.

Because the differences ΔAIC are substantial, the model, however simplified, clearly extracts nontrivial information from the data concerning the fluctuation of risk levels. Since the risk levels themselves are controlled by the estimated values of $X(t)$, as shown in Figure 1, the question then arises as to how well the values of $X(t)$ summarize in some sense the overall stress regimen at time t. It suggests that, despite the many degrees of freedom and associated complex structure, large-scale internal stress fluctuations are important aspects of the models of *Ben-Zion* [1996]. A single crude scalar measure, similar to Reid's original conception, may be sufficient to characterize periods when large events are imminent. Further examination of this question would be of interest, but it would require a comparison with the detailed stress records compiled during the original simulations and lies outside the scope of the present study.

4.2. Comparison of Model Parameters

The fitted parameters used in the calculation of the intensity functions are set out in Table 2. The main apparent differences between models lie in the values of α and ν. We proceed to a brief interpretation of the three parameters and how they may be related to the visual characteristics of the fitted intensities.

It is clear from equation (3) that e^{α} represents the initial value of the intensity $\lambda(t)$. Differences in the α values between the catalogs therefore reflect differences in the starting values; in particular, they will depend

Table 2. Fitted Parameters Using the Stress Release Model to the Synthetic Catalogs Generated by Models with Various Levels of Fault Zone Disorder[a]

Model	m_{th}	N	α	ν	ρ
U	5.0	30	-1.99	0.79	1.73
	4.5	211	0.80	0.16	2.74
F	5.0	28	0.03	0.36	1.23
	4.5	268	1.76	0.19	2.67
A	5.0	51	-0.93	0.29	2.09
	4.5	263	0.80	0.11	3.31
M	5.0	67	0.47	0.21	2.06
	4.5	358	2.02	0.06	3.67

[a]See Table 1 for details.

on where in a cycle the analysis is started. Since this is not controlled between the catalogs, the values are of no immediate importance in understanding the differences in patterns, although they do also carry some limited information about the mean intensity levels.

The fitted value of ρ estimates the rate of stress input, which is essentially dictated by the experimental set-up, which was held constant and had the same value for each of the four catalogs. It is therefore reassuring that the estimated values, though not identical, are similar in all four cases. The values increase as we drop the threshold magnitude, confirming that a significant (though not a dominant) part of the estimated stress release is occurring through events in the magnitude range $4.5 \leq m < 5$. The input rates are closer in the second analyses, suggesting that the four catalogs differ in the extent to which the stress release is achieved through the larger events; indeed, such differences are not surprising in view of the differences in the frequency-magnitude distributions from the four experiments (Figure 3).

The differences in pattern must therefore be dictated largely by the values of the remaining parameter ν, which do indeed vary systematically between the models in the expected sequence. This parameter represents the sensitivity of the risk to departures of $X(t)$ from its mean value. In the Poisson model, the risk is constant, and $\nu = 0$. The larger the value of ν, the greater the responsiveness of the risk level to changes in $X(t)$.

In fact, the values of ν vary systematically in a way

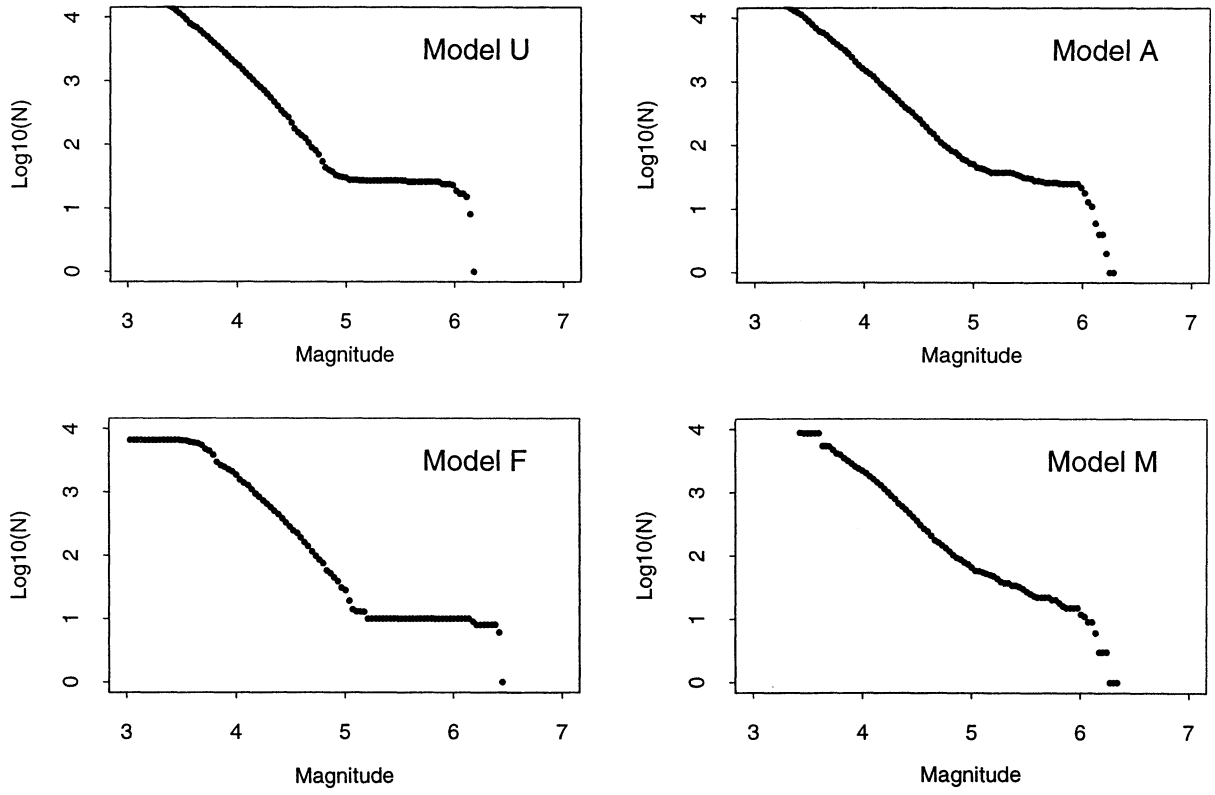

Figure 3. observed cumulative frequency-magnitude distributions during the last 100 years in the various model realizations.

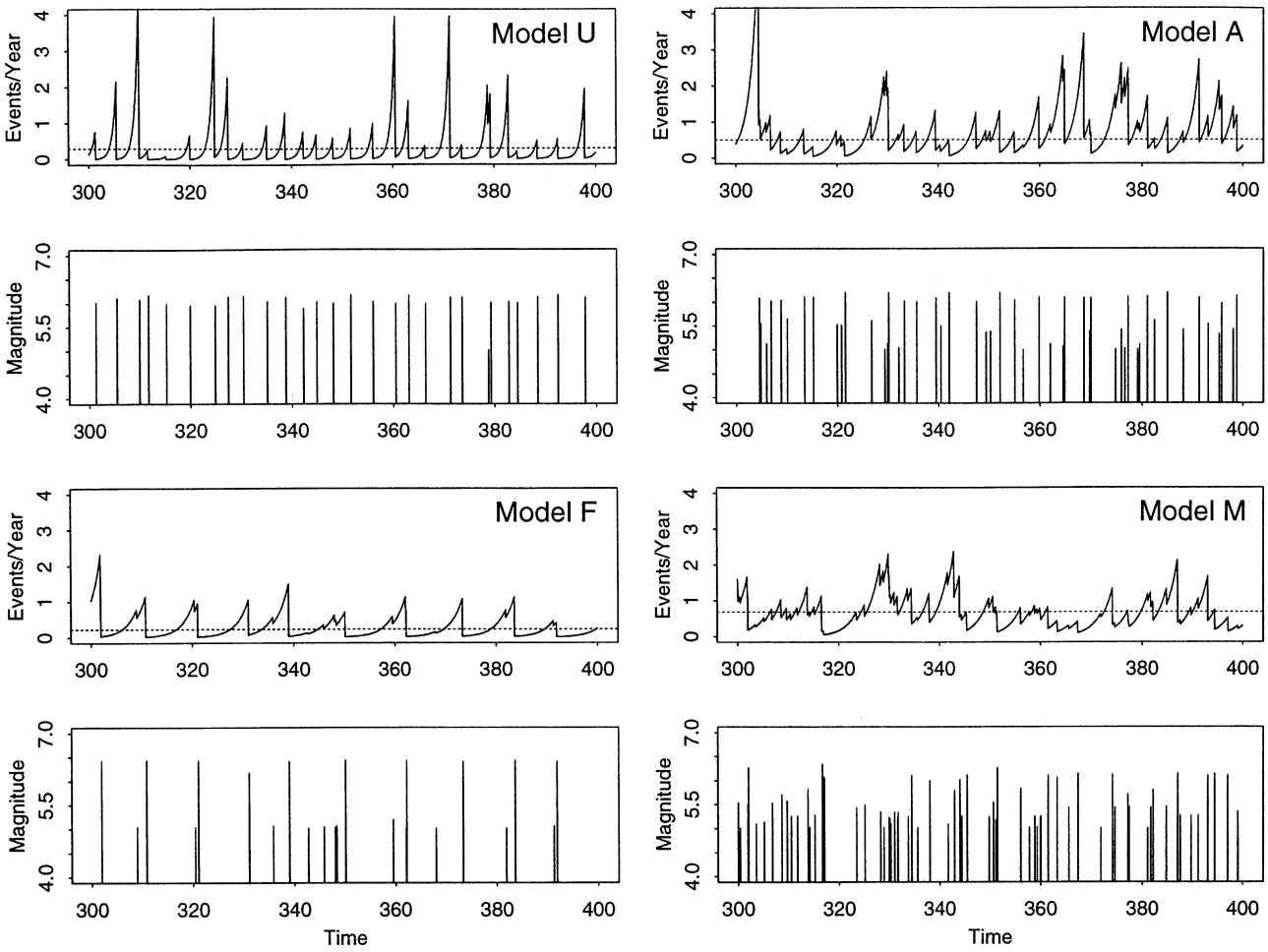

Figure 4. risk function (events/year) versus time (year) simulated by using the fitted parameters and resampling from the original distribution to obtain the magnitudes. For comparison, the simulated earthquake catalog in each case is also plotted.

which corresponds to both the visual patterns and the results of the pattern recognition studies. However, it is apparent from the simulations studied in the next section that the patterns also depend on a feature that we have so far not addressed in our discussion, namely, character of the magnitude (or stress drop) distribution. In particular, the extreme periodicity of the risk for model U seems to be caused by the combination of two features: sensitivity to the departure from the mean risk level and the near bimodal character of the magnitude distribution, which is particularly pronounced when only events with $m \geq 5$ are studied (see Figure 3). The differences in the magnitude distributions produced by the four models was one of the salient discussion points in earlier papers [*Wesnousky*, 1994; *Kagan*, 1994; *Ben-Zion and Rice*, 1995; *Ben-Zion*, 1996; *Main*, 1996]. In particular, it was suggested that the move from a distribution of traditional Gutenberg-Richter character (power law distribution for the stress drops) to one showing characteristic earthquake behavior, could be attributed to progressive changes in the character of fault heterogeneities. We found that use of the observed frequency-magnitude relations, in place of the default Gutenberg-Richter law, was essential to maintaining the character of the stress release patterns in the forward simulations described below. The effects also show up in the contrasts between the two parts of Figure 6, the first using the empirical frequency magnitude law and the second using the Gutenberg-Richter law.

The differences in visual appearance of the fitted models for the higher and lower thresholds are also interesting (compare Figures 1 and 2). The periodicity in model U is still striking, but additional features appear: there is a more obvious increase in the frequency of smaller events before a major event, and there are some apparent slower trends in the overall risk level. All plots suggest that there is more "noise" in the signal from the events with the lower threshold.

In summary, the stress release model does remarkably well, as a low-parameter statistical model, in reproducing the variety of observed patterns generated by the deterministic models with many degrees of freedom studied by *Ben-Zion and Rice* [1993, 1995]. The

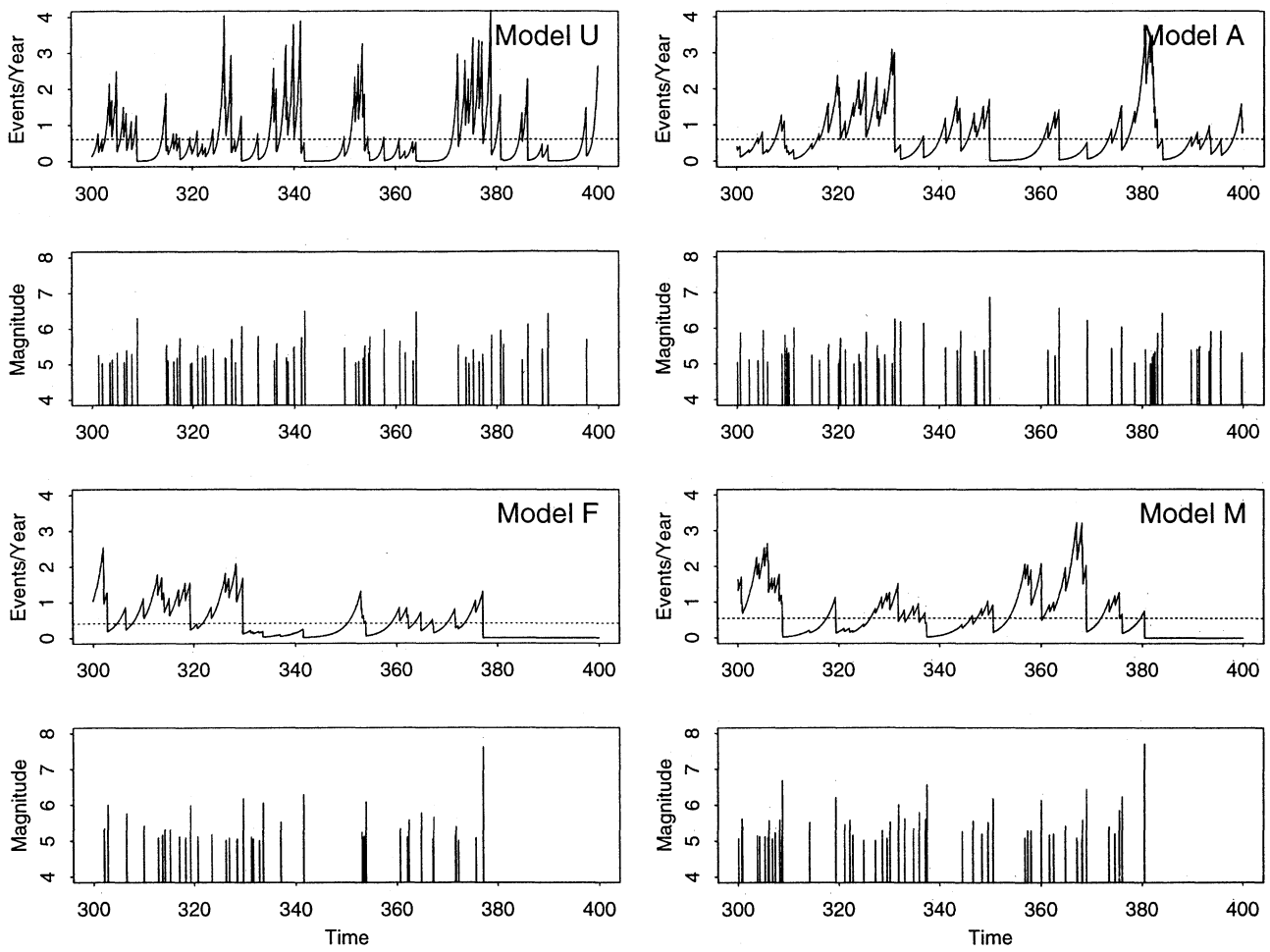

Figure 5. risk function (events/year) versus time (year) simulated by using the fitted parameters and the GR distribution with $b = 1$ to obtain the magnitudes. For comparison, the simulated earthquake catalog in each case is also plotted.

observed changes in the visual appearance of the fitted models are due to two key model parameters: the value of the parameter ν in the conditional intensity function and the character of the frequency-magnitude distribution. Changes in the parameter ν appear to be those most directly associated with the periodicity of the observed pattern, although neither characteristic by itself can fully account for the differences in the fitted patterns.

4.3. Simulations and Predictability

Using the fitted parameters, the statistical model can be used to simulate the sequence of events forward in time. Examples of such simulations, for each of the four catalogs, are shown in Figure 4 and Figure 5. Each takes the time history forward for a further 100 years, namely, over the period from $t = 300$ to $t = 400$, assuming the model parameters remain constant. By using a large number of such simulations, all based on the same past history, we can easily find the probability distribution for any quantity of interest, such as the time of the next event above a certain threshold. These are just the distributions required for probability forecasting. As an example, we shall consider the problem of predicting the time of the next event with magnitude $m \geq 6$ after the end of the data from each of the synthetic catalogs. The predictability of such an event is determined by the concentration of the distribution around its central values. Here we shall use the width of the 90% equitailed probability interval, from the fifth to the ninety-fifth percentiles, in units of the median interval, as a measure of the concentration, denoted by r_c in Table 3. To examine further the effect of the frequency-magnitude law on the predictions, we carry out the simulations, first, by using the empirical frequency-magnitude distribution for each catalog, and, second, by using a common Gutenberg Richter law, with $b = 1$ for all catalogs.

In general, the variety of data types is well reproduced by the stochastic model. Except in the case of model A, it is hard to distinguish by eye the differences between the stress patterns fitted to Ben-Zion's original data and those fitted to the simulated data (i.e.,

Table 3. Prediction Performance for the Four Models Using $m_{th} = 5$ and the Empirical or Gutenberg-Richter (GR) Distribution[a]

		Empirical Law				GR Law			
Model	m_{th}	t_m	$p_{5\%}$	$p_{95\%}$	r_c	t_m	$p_{5\%}$	$p_{95\%}$	r_c
U	5.0	4.64	2.00	8.04	1.30	20.20	4.36	55.64	2.54
	4.5	4.42	0.51	10.11	2.17	16.55	1.66	41.52	2.41
F	5.0	10.22	4.06	18.90	1.45	28.72	8.36	76.11	2.36
	4.5	10.20	2.08	22.77	2.03	17.77	3.65	47.31	2.46
A	5.0	5.10	0.62	10.92	2.02	17.43	2.00	42.84	2.34
	4.5	5.05	0.44	13.27	2.54	16.55	1.10	43.15	2.54
M	5.0	7.06	1.19	17.02	2.24	17.37	2.57	43.74	2.37
	4.5	7.63	0.79	21.89	2.76	14.07	0.83	33.40	2.31

[a]Here t_m is the mean interval defined as the ratio of the total length to the number of events with $m \geq 6.0$, and r_c is the relative concentration, i.e., $r_c = (p_{95\%} - p_{5\%})/t_m$.

between the corresponding plots in Figures 1 and 4). Spotting differences in the frequency-magnitude plots, representing the raw data, is even more difficult. The differences between the original and simulated versions of model A and, to a lesser extent, of model M are due mainly to the greater irregularity in the simulated data.

That model A should show the greatest differences may not be surprising, in that it incorporates a feature (the fixed region of high strength) which has no counterpart in the statistical model. This feature may lead to a more regular pattern of buildup of stress around the boundary of the asperity region, leading to episodes

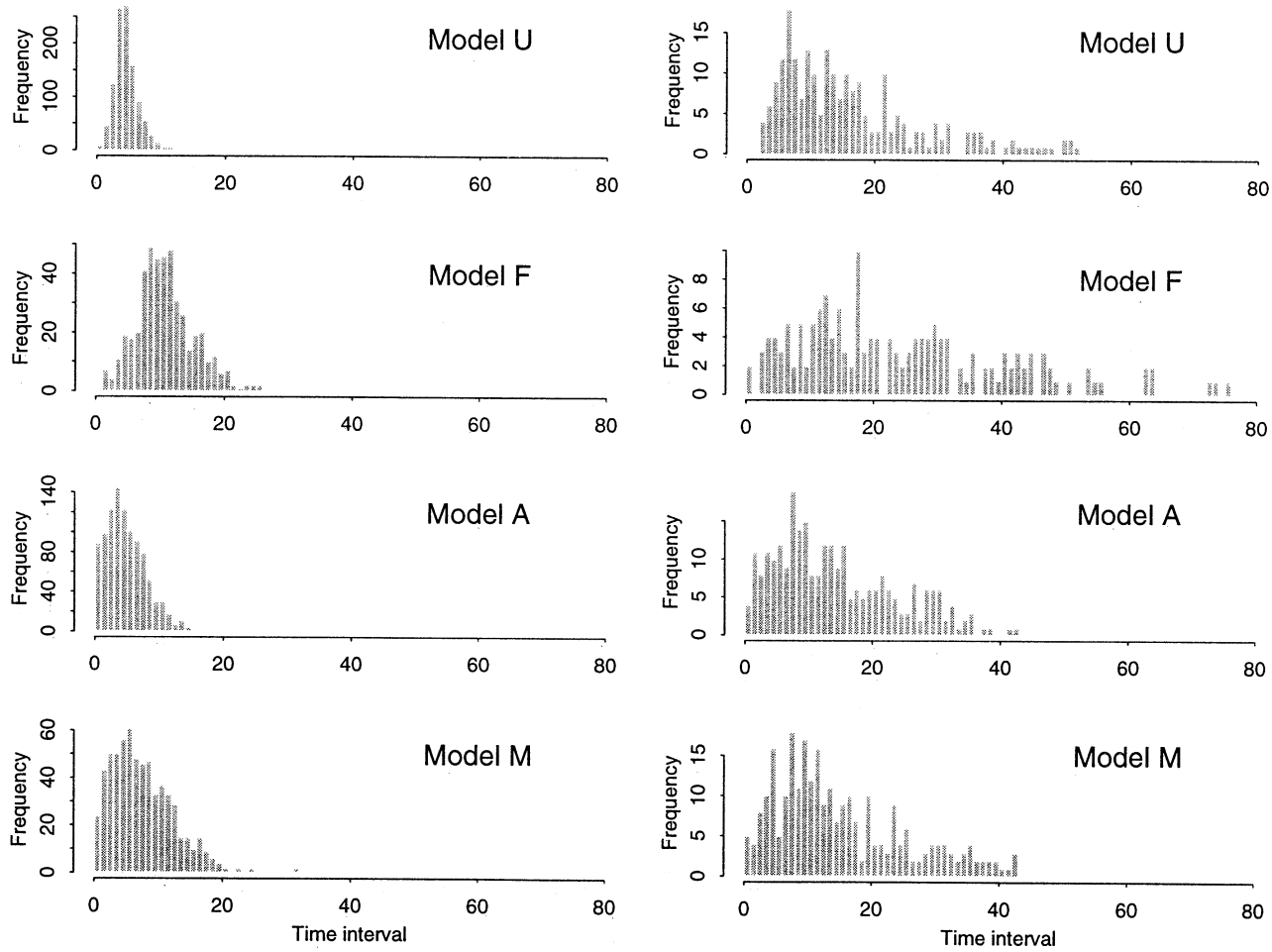

Figure 6. simulated frequency of $m \geq 6$ events for the different cases, where the left column indicates the results for the empirical distribution, and the right column for the GR distribution.

where the whole of the asperity region fails (Y. Ben-Zion, personal communication, 2000). A more complex statistical model, such as the linked stress release model explored by *Shi et al.* [1998], *Lu et al.* [1999a, 1999c], which allows for such interactions also in the statistical model, may be needed to reproduce the observed patterns more exactly.

The probability distributions for the time to the next event with $m \geq 6$ in the simulated catalogs are shown in Figure 6. Their median values may be expected to vary partly because the median time intervals between major events in the four catalogs also vary and partly because the time to the next major event will depend on the stress level when the simulations started,namely, at $t = 300$. For example, in model U, there is a large event just before the simulations start, and a dead time is to be expected before the next large event. In model M, by contrast, there is a rather high risk at the beginning of the simulation period.

The models also differ sharply in the degree of predictability, measured roughly by the ratio r_c (see Table 3). Despite the difference in initial conditions, the degree of predictability follows the same sequence as in the earlier discussions of patterns and degree of periodicity. It is of interest that the inclusion of the smaller events ($4.5 \leq m < 5$) degrades the prediction performance, suggesting again that the smaller events behave more like "noise" in relation to global risk level.

The important effect of the frequency-magnitude distribution is shown very clearly in the contrast between plots on the left and right of Figure 6. The plots on the right, using the Gutenberg Richter distribution with no cutoff at high magnitudes, show uniformly poorer predictive properties. This is chiefly because the occurrence of occasional large-magnitude events disturbs the pattern very significantly, introducing a greater degree of irregularity in the simulations.

Strictly speaking, the predictions obtained in this way only incorporate the uncertainties due to the inherent randomness of the model. In principle, additional uncertainty arises from the fact that the parameters are fitted from limited data runs and so are not known exactly. To capture this additional uncertainty, each simulation should start by first selecting parameter values from a posterior distribution for such values (see, for example, the discussion of *Vere-Jones* [1995]). This will somewhat increase the spread of the simulations and so decrease the predictability, but for simplicity, we have ignored this effect.

It is of interest to discuss two typical cases in Figure 1 from one further point of view. In model F, a fractal distribution of brittle properties with fractal dimension 2.3 is introduced. As is well known, the geometrical properties of faults can be well described by fractal sets [*Takayasu*, 1990; *Turcotte*, 1992], and so it may be reasonable to treat the stress as a global value for the region as a whole, although some further examination of the global stress at different scales may be needed. In model M with multi-size-scale heterogeneities, it is less reasonable to treat the stress as having a global character. Here, stress adjustment and redistribution between different parts of the region may be important. For example, the competition between local strengthening and weakening through interactions of tectonic stress may trigger earthquakes at a long distance from the origin event. In such cases, the simple model is less effective, and more parameters may be needed in order to describe the effects of spatial heterogeneities, as indicated by [*Lu et al.* 1999a, 1999c], and to maintain a common degree of predictability. *Steacy et al.* [1996] also noted the relation between the disorder characterizing fault properties and the level of earthquake complexity. In such situations, it is useful to regulate the number of parameters by a procedure such as AIC, which is related in its derivation to the degree of predictability mentioned above.

5. Conclusions

In this paper, the stress release model, a simple stochastic version of the elastic rebound model, is applied to the larger events within synthetic earthquake catalogs generated by models with various levels of fault zone disorder. Simulations show that the model succeeds remarkably well in reproducing the range of data types arising from the four cases studied. The model parameters affecting the degree of periodicity have been isolated and indicate an important role of the frequency-magnitude distribution. The model allows important characteristics of the global risk level to be predicted probabilistically, without requiring detailed knowledge of the system. Based on both the AIC and simulations, the results show that the degree of regularity or predictability of large events for the assumed fault properties follows the order U, F, A, and M, which is consistent with that obtained previously by pattern recognition techniques. The effect of the heterogeneity of the fault surface properties on time-dependent seismic hazard calculation is further highlighted. Varying the lower-magnitude threshold for the events entering into the study suggests that the larger events are more predictable than the smaller ones and that the smaller ones play a relatively minor role in determining the global risk levels. Further analysis, using something like a linked stress release model, would be needed to understand more clearly the role of the smaller events in building up and releasing local risk level.

Acknowledgments. The authors are grateful to Yehuda Ben-Zion for kindly supplying the synthetic earthquake catalogs and to David Harte, Mark Bebbington, Hideki Takayasu, Yehuda Ben-Zion, and Yaolin Shi for many valuable discussions and assistance. Constructive and insightful comments by Marian Anghel, Mariana Eneva, and associate editor Yehuda Ben-Zion largely improved the manuscript. This work was supported by the Marsden Fund administered by the Royal Society of New Zealand.

References

Akaike, H., On entropy maximization principle, in *Applications of Statistics,* edited by P. R. Krishnaiah, pp. 27-41, North-Holland, New York, 1977.

Bebbington, M., A hierarchical stress release model for synthetic seismicity, *J. Geophys. Res., 102,* 11,677-11,687, 1997.

Ben-Zion, Y., Stress, slip, and earthquakes in models of complex single-fault systems incorporating brittle and creep deformations, *J. Geophys. Res., 101,* 5677-5706, 1996.

Ben-Zion, Y., and J. R. Rice, Earthquakes failure sequences along a cellular fault zone in a three-dimensional elastic solid containing asperity and nonasperity regions, *J. Geophys. Res., 98,* 14,109-14,131, 1993.

Ben-Zion, Y., and J. R. Rice, Slip patterns and earthquake populations along different classes of faults in elastic solids, *J. Geophys. Res., 100,* 12,959-12,983, 1995.

Di Luccio, F., R. Console, M. Imoto, and M. Murru, Analysis of short time-space range seismicity patterns in Italy, *Ann. Geofis., 40,* 783-798, 1997.

Eneva, M., and Y. Ben-Zion, Techniques and parameters to analyze seismicity patterns associated with large earthquakes, *J. Geophys. Res., 102,* 17,785-17,795, 1997a.

Eneva, M., and Y. Ben-Zion, Application of pattern recognition techniques to earthquake catalogs generated by model of segmented fault systems in three-dimensional elastic solids, *J. Geophys. Res., 102,* 24,513-24,528, 1997b.

Harte, D., Documentation for the statistical seismology library, *Rep. 10* 101pp., Sch. of Math. and Comput. Sci., Victoria Univ. of Wellington, Wellington, New Zealand, 1998.

Kagan, Y. Y., Observational evidence for earthquakes as a non-linear dynamic process, *Physica D, 77,* 160-192, 1994.

Kagan, Y. Y., and L. Knopoff, Earthquake risk prediction as a stochastic process, *Phys. Earth Planet. Inter., 14,* 97-108, 1977.

Kanamori, H., and D. L. Anderson, Theoretical basis of some empirical relations in seismology, *Bull. Seismol. Soc. Am., 65,* 1073-1095, 1975.

Knopoff, L., A stochastic model for the occurrence of main-sequence earthquakes, *Rev. Geophys., 9,* 175-188, 1971.

Lu, C., D. Harte, and M. Bebbington, A linked stress release model for historical Japanese earthquakes: Coupling among major seismic regions, *Earth Planets Space, 51,* 907-916, 1999a.

Lu, C., D. Vere-Jones, and H. Takayasu, Avalanche behavior and statistical properties in a microcrack coalescence process, *Phys. Rev. Lett., 82,* 347-350, 1999b.

Lu, C., D. Vere-Jones, H. Takayasu, A. Yu. Tretyakov, and M. Takayasu, Spatio-temporal seismicity in an elastic block lattice model, *Fractals, 7,* 301-311, 1999c.

Main, I., Statistical physics, seismogenesis, and seismic hazard, *Rev. Geophys., 34,* 433-462, 1996.

Main, I., T. Leonard, O. Papasouliotis, C. G. Hatton, and P. G. Meredith, One slope or two? Detecting statistically significant breaks of slope in geophysical data, with application to fracture scaling relationships, *Geophys. Res. Lett., 26,* 2801-2804, 1999.

Reid, H. F., The elastic-rebound theory of earthquakes, *Univ. Calif. Publ. Geol. Sci., 6,* 413-444, 1911.

Shi, Y., J. Liu, D. Vere-Jones, J. Zhuang, and L. Ma, Application of mechanical and statistical models to study of seismicity of synthetic earthquakes and the prediction of natural ones, *Acta Seismol. Sinica, 11,* 421-430, 1998.

Steacy, S. J., J. McCloskey, C. J. Bean, and J. Ren, Heterogeneity in a self-organized critical earthquake model, *Geophys. Res. Lett., 23,* 383-386, 1996.

Takayasu, H., *Fractals in the Physical Sciences,* 170 pp., Manchester Univ. Press, Manchester, England, 1990.

Turcotte, D. L., *Fractals and Chaos in Geology and Geophysics,* 221 pp., Cambridge Univ. Press, New York, 1992.

Vere-Jones, D., Earthquake prediction: A statistician's view, *J. Phys. Earth, 26,* 129-146, 1978.

Vere-Jones, D., Forecasting earthquakes and earthquake risk. *Int. J. Forecasting, 11,* 503-538, 1995.

Vere-Jones, D., Probabilities and information gain for earthquake forecasting, *Comput. Seismol., 30,* 249-263, 1998.

Vere-Jones, D., and Y. L. Deng, A point process analysis of historical earthquakes from North China, *Earthquake Res. China, 2,* 165-181, 1988.

Wesnousky, S. G., The Gutenberg-Richter or characteristic earthquake distribution, which is it?, *Bull. Seismol. Soc. Am., 84,* 1940-1959, 1994.

Zheng, X., and D. Vere-Jones, Application of stress release models to historical earthquakes from North China. *Pure Appl. Geophys., 135,* 559-576, 1991.

Zheng, X., and D. Vere-Jones, Further applications of the stochastic stress release model to historical earthquake data, *Tectonophysics, 229,* 101-121, 1994.

C. S. Lu and D. Vere-Jones, School of Mathematical and Computing Sciences, Victoria University of Wellington, Wellington 600, New Zealand. (cslu@mcs.vuw.ac.nz; dvj@mcs.vuw.ac.nz)

(Received May1, 2000; revised November 21, 2000; accepted November 30, 1000.)